DNS of a Turbulent Premixed Jet Flame with Fully Developed Turbulent Inlet

M.C. Ma, M. Talei, and R.D. Sandberg

Department of Mechanical Engineering
University of Melbourne, Victoria 3000, Australia

Abstract

A Direct Numerical Simulation (DNS) study is conducted of a premixed round jet flame with a fully turbulent flow exiting a long pipe as inlet condition. The inclusion of the pipe in the simulation with a fully turbulent flow inside ensures that the turbulence-flame interaction, in particular near the inlet region, is well represented. The orientation of turbulence structures in different regions of the domain is identified. The interaction between the turbulence structures and the flame is examined using vector alignments. Streamwise oriented vortical structures formed in the pipe boundary layer are convected into the base of the flame. Preferential alignment of the flame normal with the compressive eigenvector of the strain rate tensor is observed close to the pipe exit suggesting that the turbulence characteristics of the jet inlet have an effect on the flame front close to the flame base.

Introduction

Turbulent reacting flows play a prominent role in many important engineering applications in the energy and transportation fields. Understanding how turbulence and combustion influence each other is important in helping to design safer, cleaner and more efficient combustion systems. High-fidelity simulations provide a way to obtain invaluable datasets to study flame-turbulence interactions. However, due to the wide range of length and time scales present in turbulent flames, it is still computationally infeasible to conduct simulations without making compromises in certain aspects. This includes reducing the complexity in the chemistry model, lowering the Reynolds number, or simplifications in the flow geometry. The simplification of the inflow boundary conditions is one of the approaches often invoked to reduce the computational cost. For example, the inflow for a jet flame would be imposed at the plane of the flame base. Commonly, DNS studies focus on analysing regions away from the inlet, with the assumption that the regions are sufficiently far and therefore the uncertainty related to inlet boundary conditions are minimal. However, DNS data with better established upstream regions is lacking, but can be valuable for analysis of upstream physics, as well as for comparison to RANS/LES and experimental studies which investigate these regions.

Some numerical studies have shown that flow characteristics in the upstream region are influenced by the quality of turbulence generation method used at the inlet, as methods of generating synthetic turbulence vary in complexity, cost, and accuracy. Sandberg *et al.* [8] presented a DNS study of a non-reacting jet with a fully developed inflow generated by the inclusion of a long pipe and found trailing edge effects at the nozzle exit affects the turbulence statistics. Additionally, the nozzle lip had an impact on the acoustic field. Herff *et al.* [3] also suggested that synthetic inflow boundary conditions in cold jets result in under-prediction of the turbulent kinetic energy due to the missing acoustic modes in the nozzle. Scalar profiles are also often prescribed in the absence of geometric representation featuring separate streams of reactants and products.

In turbulent premixed combustion, turbulence has a significant impact on the flame dynamics, such as flame straining, curvative, and flame propagation speed. Vortical structures are known to wrinkle the flame surface and increase local concave scalar structures [1]. The flame also subsequently affects the evolution of the turbulence, where vortical structures become weaker as they move towards the hot gases due to viscous dissipation. DNS studies of turbulence-flame interactions in flows with shear-driven turbulence, such as jets, generally use synthetic turbulent inflow at the base of the flame and have reported laminar-like flame features in the near nozzle region [10, 9]. Near nozzle effects are especially important when investigating various phenomena such as flame base stability and noise generation.

In the current paper, Direct Numerical Simulation (DNS) of a premixed round jet flame is performed. The DNS consists of a pipe issuing unburned gases into an open environment. The pipe is sufficiently long such that the turbulent flow is fully developed. The turbulence and flame characteristics near the pipe exit region are analysed. The aim is to provide insight into the turbulence and flame dynamics under a more accurate representation of the turbulent structures near the flame base.

Numerical Methods and Setup

The non-dimensionalized compressible Navier-Stokes and scalar transport equations for the reactant mass fraction Y_R are solved in cylindrical coordinates using the highly-optimized code HiPSTAR to simulate a statistically stationary methane-air premixed jet flame. HiPSTAR is a hybrid MPI/OpenMP computational fluid dynamics solver originally developed to simulate compressible turbulent flows, with its capabilities extended to simulate reacting flows in the current study by implementing a single step chemistry model. Numerous published studies have been conducted with the code for non-reacting flows [8], and this study is the first application of combustion using HiPSTAR. The code has been validated on various reacting test cases. The streamwise and radial directions are discretized using a fourth-order standard-finite difference scheme. A spectral method by Fourier decomposition is used in the azimuthal direction. Time marching is accomplished by a low-storage fourth-order Runge-Kutta scheme.

The computational domain consists of seven blocks to represent the pipe, flame region downstream of the pipe exit, and the far-field. A sketch of the computational domain is shown in figure 1. A preheated unburnt mixture ($Y_R = 1$) of equivalence ratio $\Phi = 1$, with temperature of $T = 800K$ is introduced. The jet Reynolds number based on the pipe diameter is $Re = 10,000$. A hot co-flow of burnt gas ($Y_R = 0$) has a temperature of $2460K$ with a velocity of 1% of the jet bulk velocity. The flame is anchored at the pipe wall lip with the temperature profile of a laminar flame front specified across the width of the lip. The unstretched laminar flame speed non-dimensionalized by the inlet mean velocity is $S_L/U = 0.00829$. The Damkohler number defined by $Da = D_o B_o/S_L^2 \exp(\beta/\alpha)$ is 93.597, where D_o is the diffusion coefficient, B_o is the pre-exponential factor, α is the heat release rate, and β is the dimensionless activation en-
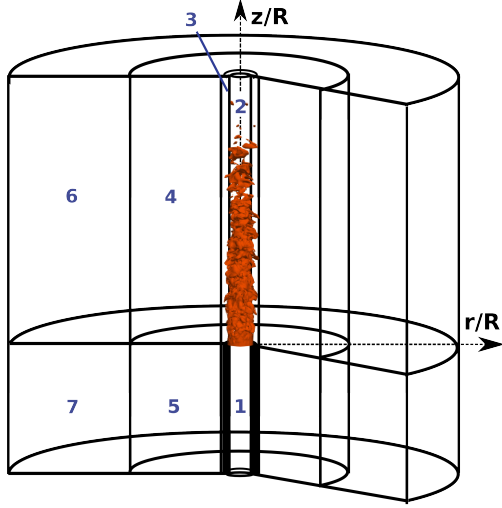
Figure 1: Sketch of seven block computational domain (not to scale).

ergy. The Mach number based on jet bulk velocity is 0.35. A single-step irreversible chemistry model is used for the chemical source term in the scalar equation to reduce the computational cost. The flame parameters are summarised in table 1.

The digital filter technique, which is capable of correlating the length scales of the flow, is used for pipe inflow turbulence generation [5] in block 1. Sandberg *et al.* [8] found that an adaptation length of approximately 35-40 radii was sufficient to establish a fully developed turbulent pipe flow using this inflow method. The imposed inlet mean velocity profile is obtained from a precursor periodic pipe simulation at the same Reynolds number and Mach number. A laminar boundary layer inlet is imposed at the coflow inlet in blocks 5 and 7. Non-reflecting characteristic boundary conditions are used at the outermost radial boundary and at the furthest downstream boundary. An axis treatment based on parity conditions is imposed [7]. A uniform streamwise grid spacing of $\Delta z/D = 0.00875$ is used from the pipe exit $z/D = 0.0$ to $z/D = 25$ to resolve the flame region. Outside this fine region, polynomial grid stretching is applied. The azimuthal direction is resolved with 192 Fourier modes in blocks 1-4, and with 32 modes in block 5. The acoustic field is resolved up to 8 Fourier modes in blocks 6 and 7. The lengths, number of grid points, and number of azimuthal modes are summarized in table 2. The simulation was performed for 8 jet flow-through times to achieve statistical convergence.

Results

In figure 2, instantaneous contours of vorticity magnitude are shown along with an iso-contour $Y_R = 0.134$ to represent the

Block	$L_z \times L_r$	$N_z \times N_r$	k/nzp
1	50.0×1.0	560×75	$192/386$
2	60.0×1.0	2000×75	$192/386$
3	60.0×0.1	2000×25	$192/386$
4	60.0×7.0	2000×200	$192/386$
5	50.0×7.0	480×200	$32/66$
6	60.0×37.0	2000×300	$8/18$
7	50.0×37.0	480×300	$8/18$

Table 2: Lengths, grid points, and Fourier modes (k)/collocation points (nzp) for each block in the computational domain as depicted in figure 1. All dimensions are normalized with the pipe radius R.

flame front, where the value of Y_R is associated with peak reaction rate in the unstretched laminar flame. High vorticity regions can be observed close to the pipe wall due to high velocity gradients. These regions continue beyond the pipe exit where they interact with the flame front anchored at the pipe exit. In the jet, the regions with highest values of vorticity can be observed in the shear layer. The shear layer closely coincides with the flame front near the pipe exit. Further downstream, the shear layer continues to expand radially while the flame shows an opposite behaviour. Smaller regions of high vorticity values are also observed in the jet core. Downstream of the flame, the vortical structures in the core are not found, due to rapid dissipation by the increased viscosity in the burnt gas. This is in contrast to the vorticity field of a non-reacting jet, where there is no rapid dissipation of vorticity [8].

To better visualize the three-dimensional vortical structures, they can be represented by iso-surfaces of the swirling strength criterion λ_{ci} [11]. Figure 3a and 3b show iso-surfaces of $\lambda_{ci} = 1.25$ near the pipe exit (up to $z/R = 3$) and further downstream (from $z/R = 3$ to 10), respectively. Additionally, the iso-surfaces of a non-reacting jet from the study of Sandberg *et al.* [8] is shown in figures 3c and 3d for the same respective axial locations. In figure 3a and 3c, long streamwise structures are observed in the pipe flow for both the reacting and non-reacting cases, respectively. In contrast, the jet shows spanwise oriented horseshoe vortex structures formed by the shear layer between the high velocity jet and low velocity coflow. Comparing figures 3b and 3d, a clear difference is observed between the reacting and non-reacting jets in the downstream locations. The non-reacting jet show similar vortical structures at different the streamwise locations. In the reacting jet, many of the vortical structures decay shortly after leaving the pipe exit, while some elongated structures appear. As observed in figure 2a, the structures from the core of the jet are expected to be dampened by the high viscosity of the flame and surrounding hot gas. The elongated structures on the other hand, appear to form outside the flame and are orientated in the streamwise directions. Similar structures were observed by Duwig and Dunn [2] in an LES simulation of a premixed flame. It is likely that the formation of these elongated structures are due to the difference between the increased radial and azimuthal components of velocity originating from the flame, and the streamwise velocity of the co-
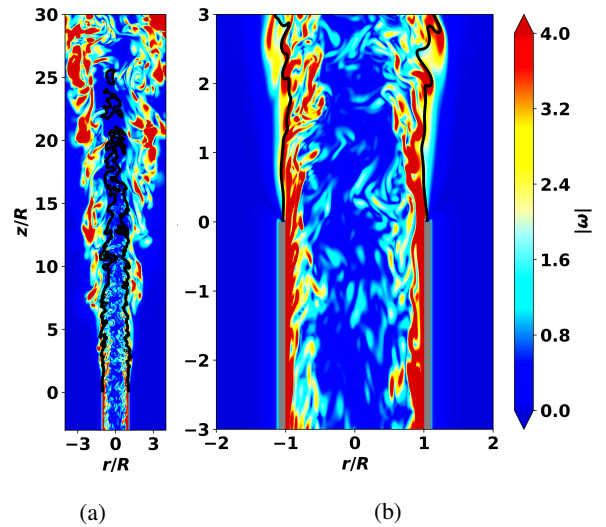

(a)   (b)

Figure 2: Instantaneous contours of the vorticity magnitude and $Y_R = 0.134$ iso-surface (black line) (a) with view of entire flame and surrounding field, and (b) in the region of the pipe exit.

Φ	Re	S_L/U_b	α	Da
1.0	10000	0.00829	0.675	93.597

Table 1: Flame parameters.

flowing hot gas.

The average spatial orientations of structures are further investigated by the variable Γ defined as [4]

$$\Gamma = \frac{\overline{p_z p_z} - \overline{p_\theta p_\theta}}{\overline{p_z p_z} + \overline{p_\theta p_\theta}} , \qquad (1)$$

where $p_z = \partial p/\partial z$ and $p_\theta = \partial p/\partial \theta$ are the streamwise and spanwise partial pressure derivatives respectively. $\Gamma = 1$ indicates that streamwise gradients are dominant and structures are orientated in the spanwise direction, while $\Gamma = -1$ indicated that spanwise gradients are dominant and structures are orientated in the streamwise direction. Figure 4 shows the spanwise averaged field of Γ with an iso-contour of of $\widetilde{Y_R} = 0.134$ shown with a black line. Also shown are the radial profiles of Γ in the pipe one diameter upstream from the pipe exit and at downstream locations $z/L_f = 1/32, 1/8$, and $1/2$, where the flame length L_f is approximately 11 diameters measured from the flame base to the most downstream location of $\widetilde{Y_R} = 0.134$. In the near wall regions of the pipe, the structures are strongly streamwise oriented, indicated by the negative values of Γ up to $\Gamma = -0.5$.
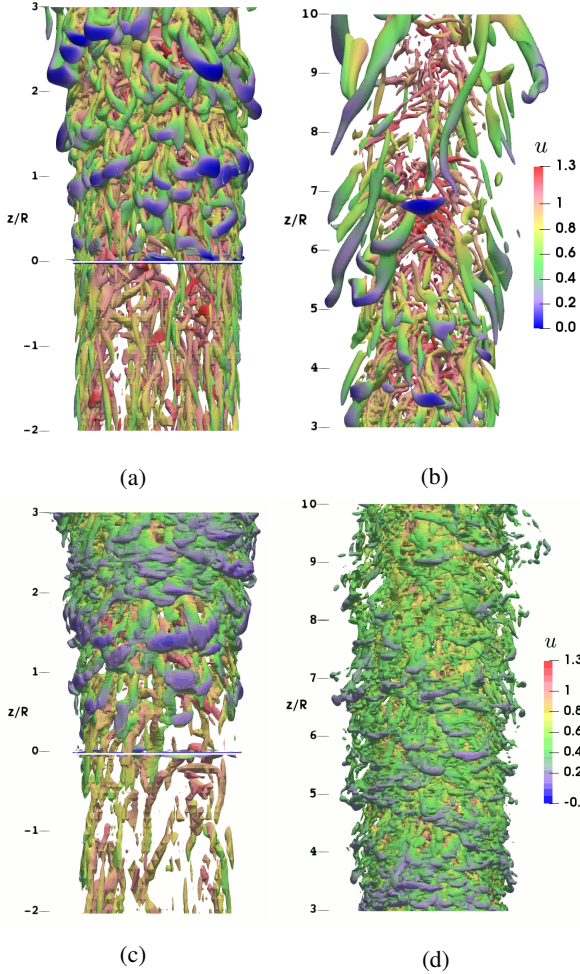

(a)   (b)

(c)   (d)

Figure 3: Instantaneous iso-surfaces of $\lambda_{ci} = 1.25$ for the (a,b) flame and (c,d) a non-reacting jet [8], coloured by velocity.

Further downstream at $z/L_f = 1/8$ and $z/L_f = 1/2$ values of Γ are in the range of $0 < \Gamma < 0.25$ in core of the flame, indicating a slight preference towards spanwise oriented structures. The shear layer of the jet is largely spanwise structure dominated with high positive values of Γ. It can be observed at $z/L_f = 1/32$ that the region of dominant streamwise structure close to the pipe wall extends for a small distance downstream of the nozzle lip, indicating that the flame starts to influence these structures as they convect further. It is also noted that further downstream, the Γ field can be separated into three regions: the slightly positive regions in the reactant side of the flame, the highly positive region in the shear layer, and a region in between with negative values of Γ. This third region is consistent with the elongated structure observed in figure 3b.
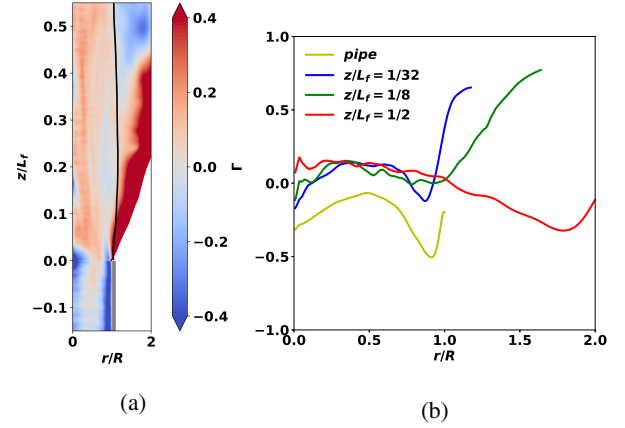

(a)   (b)

Figure 4: (a) Spanwise average of Γ with black line denoting the flame front based on iso-contour of $\widetilde{Y_R} = 0.134$ (b) profiles of Γ at four streamwise locations. Regions with turbulence intensity $< 1\%$ are filtered.

To investigate the interaction from the vortex structures with the flame, alignment statistics are considered. The focus here is on the alignment between the vorticity vector $\omega = \nabla \times \mathbf{u}$, flame normal vector $\mathbf{n} = -\nabla Y_R/|\nabla Y_R|$ describing the orientation of the flame front, and the eigenvectors $\mathbf{e}_1$, $\mathbf{e}_2$, and $\mathbf{e}_3$ of the strain rate tensor. Statistics are conditioned on the flame front represented by $Y_R = 0.134$ and reported for the streamwise locations $z/L_f = 1/32, 1/8$, and $1/2$. The PDF of alignments between the flame normal, $\mathbf{n}$, and the vorticity vector ω are shown in figure 5. The PDFs show the expected behaviour where $\mathbf{n}$ is misaligned with ω, such that the vorticity vector aligns with the tangent of the flame front. The misalignment is the strongest for $z/L_f = 1/32$ and $1/8$.

The PDF of alignments between the flame normal, $\mathbf{n}$, and strain rate eigenvectors, $\mathbf{e}_{1,2,3}$, are shown in figure 6. For an isotropic flow, the flame normal vector most preferentially aligns with the eigenvector associated with the smallest eigenvalue, which is identified as the compressive eigenvector $\mathbf{e}_3$, while the flame front tangent aligns with the extensive eigenvector $\mathbf{e}_1$. The alignment of the flame normal with the compressive eigenvector increases the Y_R gradient [6], creating locally thinner flame fronts. Wang *et al.* [9] observed that close to the inflow boundary, $|\mathbf{n} \cdot \mathbf{e}_1|$ and $|\mathbf{n} \cdot \mathbf{e}_3|$ had similar PDFs, showing an angle of 45 degree between $\mathbf{n}$ and $\mathbf{e}_1/\mathbf{e}_3$. This was attributed to a laminar
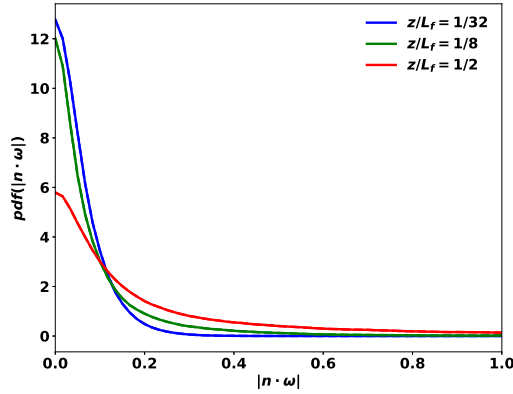
Figure 5: PDFs of alignment between the flame normal vector and vorticity vector at $z/L_f = 1/32$ (solid), $z/L_f = 1/8$ (solid), $z/L_f = 1/2$ (dotted).

like flame front. The increase in $|\mathbf{n} \cdot \mathbf{e}_3|$ and decrease in $|n \cdot \mathbf{e}_1|$ with axial distance indicate increasing dependence of the flame front to turbulence. In the present flame, the PDFs of $|\mathbf{n} \cdot \mathbf{e}_1|$ and $|\mathbf{n} \cdot \mathbf{e}_3|$ are offset even at the upstream location, suggesting that the influence of turbulence on wrinkling the flame front occurs even close to the pipe exit. With increasing axial distance, the behaviour of the alignments are consistent with the observations in other DNS studies, where the flame normal is more aligned with the most compressive eigenvector.
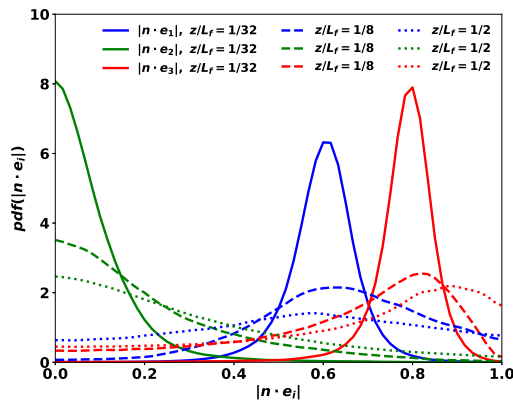

Figure 6: PDFs of alignment between the flame normal and strain rate eigenvectors at $z/L_f = 1/32$ (solid), $z/L_f = 1/8$ (solid), $z/L_f = 1/2$ (dotted).

Conclusions

A DNS study of a turbulent premixed jet flame of $Re = 10,000$ with fully developed turbulent inflow was conducted by including a long pipe section. The inclusion of the pipe provides a more realistic representation of the flame inlet turbulence. A strong vorticity field was present in the jet shear layer. Streamwise vortical structures were found to form in the pipe boundary layer and were subsequently convected into the flame. Further downstream, the spanwise oriented vortical structures are more favoured in the vicinity of the flame front. Also, the presence of some elongated streamwise structures outside the flame was evident. The flame normal is strongly misaligned with the vorticity vector, consistent with what previously reported in the literature. It was also observed that the preferential alignment of the flame normal with the most compressive eigenvector of the

strain rate tensor is even at upstream locations suggesting that turbulence has an important influence on the flame front close to the flame base.

References

[1] Cifuentes, L., Dopazo, C., Martin, J., Domingo, P. and Vervisch, L., Effects of the Local Flow Topologies Upon the Structure of a Premixed Methane-air Turbulent Jet Flame, *Flow Turbulence Combust*, **96**, 2016, 535–546.

[2] Duwig, C. and Dunn, M. J., Large Eddy Simulation of a Premixed Jet Flame Stabilized by a Vitiated Co-flow : Evaluation of auto-ignition tabulated chemistry, *Combustion and Flame*, **160**, 2013, 2879–2895.

[3] Herff, S., Pausch, K., Nawroth, H., Schlimpert, S., Paschereit, C. O. and Schröeder, W., Impact of Turbulent Inflow Distributions on Combustion Noise of Lean-Premixed Flames, in *23rd AIAA/CEAS Aeroacoustics Conference*, 2017.

[4] Jones, L. E. and Sandberg, R. D., Acoustic and hydrodynamic analysis of the flow around an aerofoil with trailing-edge serrations, *Journal of Fluid Mechanics*, **706**, 2012, 295–322.

[5] Klein, M., Sadiki, A. and Janicka, J., A Digital Filter based Generation of Inflow Data for Spatially Developing Direct Numerical or Large Eddy Simulations, *Journal of Computational Physics*, **186**, 2003, 652–665.

[6] Nilsson, T., Carlsson, H., Yu, R. and Bai, X.-S., Structures of Turbulent Premixed Flames in the High Karlovitz Number Regime DNS Analysis, *Fuel*, **216**, 2018, 627–638.

[7] Sandberg, R. D., An Axis Treatment for Flow Equations in Cylindrical Coordinates Based on Parity Conditions, *Computers and Fluids*, **49**, 2011, 166–172.

[8] Sandberg, R. D., Sandham, N. D. and Suponitsky, V., DNS of Compressible Pipe Flow Exiting into a Coflow, *International Journal of Heat and Fluid Flow*, **35**, 2012, 33–44.

[9] Wang, H., Hawkes, E. R. and Chen, J. H., Turbulence-flame Interactions in DNS of a Laboratory High Karlovitz Premixed Turbulent Jet Flame, *Physics of Fluids*, **28**, 2016, 095107.

[10] Wang, H., Hawkes, E. R., Zhou, B., Chen, J. H., Li, Z. and Aldén, M., A Comparison Between Direct Numerical Simulation and Experiment of the Turbulent Burning Velocity-related Statistics in a Turbulent Methane-air Premixed Jet Flame at High Karlovitz Number, *Proceedings of the Combustion Institute*, **36**, 2017, 2045–2053.

[11] Zhou, J., Adrian, R. J., Balachandar, S. and Kendall, T. M., Mechanisms for Generating Coherent Packet of Hairpin Vortices in Channel Flow, *Journal of Fluid Mechanics*, **387**, 1999, 353–396.